BIOCHEMISTRY
including biophysical chemistry & molecular biology

Article

pubs.acs.org/biochemistry

Biomimetic Environment to Study *E. coli* Complex I through Surface-Enhanced IR Absorption Spectroscopy

Sébastien Kriegel,[†] Taro Uchida,[‡] Masatoshi Osawa,[‡] Thorsten Friedrich,[§] and Petra Hellwig*[,†]

[†]Laboratoire de bioelectrochimie et spectroscopie, UMR 7140, Chimie de la Matière Complexe, Université de Strasbourg-CNRS, Strasbourg 67000, France

[‡]Catalysis Research Center, Hokkaido University, Sapporo 001-0021, Japan

[§]Institut für Biochemie, Albert-Ludwigs-Universität Freiburg, Albertstrasse 21, 79104 Freiburg im Breisgau, Germany

Supporting Information

ABSTRACT: In this study complex I was immobilized in a biomimetic environment on a gold layer deposited on an ATR-crystal in order to functionally probe the enzyme against substrates and inhibitors via surface-enhanced IR absorption spectroscopy (SEIRAS) and cyclic voltammetry (CV). To achieve this immobilization, two methods based on the generation of a high affinity self-assembled monolayer (SAM) were probed. The first made use of the affinity of Ni-NTA toward a hexahistidine tag that was genetically engineered onto complex I and the second exploited the affinity of the enzyme toward its natural substrate NADH. Experiments were also performed with complex I reconstituted in lipids. Both approaches have been found to be successful, and electrochemically induced IR difference spectra of complex I were obtained.

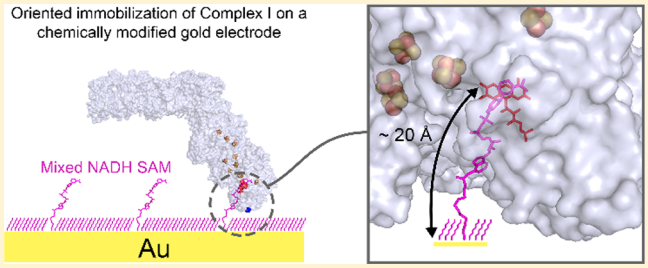

INTRODUCTION

The energy-converting NADH:ubiquinone oxidoreductase, respiratory complex I, is the main entrance for electrons of many respiratory chains establishing the proton motive force required for energy consuming processes. Complex I is a membranous enzyme complex with a molecular mass of approximately 520 kDa in prokaryotes and about 980 kDa in mitochondria.[1−3] The complex has an unusual two-part structure consisting of a peripheral arm extending into the aqueous phase and a membrane arm embedded in the lipid bilayer. All redox cofactors, namely, one noncovalently bound flavin mononucleotide (FMN) and depending on the organism up to 10 iron−sulfur (Fe−S) clusters, are located within the peripheral arm.

The structure of the complex from *Thermus thermophilus* was recently resolved at 3.3 Å resolution.[4] In addition, the structure of the mitochondrial complex from *Yarrowia lipolytica* at 6.3 Å resolution was published.[5] From these data and other biochemical evidence a model was developed in which conformational changes brought about by the redox reaction in the peripheral arm are proposed to be transmitted to four proton channels in the membrane arm by a central hydrophilic axis assisted by a 140 Å long α-helix and a 160 Å long ß-hairpin helix element. The latter two unique structural elements both align parallel to the membrane arm and are located toward its cytoplasmic and the periplasmic side, respectively.

In order to probe the conformational reorganization of the membrane arm by spectroscopic techniques it is crucial to develop an experimental approach that allows studying the coupled electron and proton translocation in a biomimetic environment, ideally on an electrode in order to induce the electron transfer. Numerous strategies for the immobilization of proteins on surfaces are found in the literature.[6−11] Here, we focus on the adsorption of proteins on a gold surface, since this can subsequently be used in surface-enhanced infrared absorption spectroscopic (SEIRAS)[12] and electrochemical experiments, such as cyclic voltammetry (CV). To avoid protein denaturation, the metal surface is often coated with a layer of organic molecules, for example, by using a thiol-based self-assembled monolayer (SAM). Depending on the desired orientation of a protein, the polarity and the morphology of the SAM/surface are modulated by choosing different thiol-containing compounds and by adapting the nanostructure of the gold film. Once a SAM is formed, it can be further modified by chemical reactions. The number of surfaces hereby generated is virtually unlimited. To determine the influences of the SAM and the surface on the properties of a redox enzyme, numerous studies used the soluble electron carrier cytochrome *c* as a model,[13] as this enzyme is small (~13 kDa), and heme *c*, its only redox cofactor, readily transfers electrons to and from the protein surface. For example, when the alkanethiol used to create the SAM contains fewer than ~10 methylene groups, electron tunneling from the electrode to the enzyme is rapid and not rate limiting. Also, the electrostatic

Received: August 1, 2014
Revised: September 12, 2014
Published: September 16, 2014

   dx.doi.org/10.1021/bi500955a | *Biochemistry* 2014, 53, 6340−6347

properties of the SAM are important; a SAM of 11-mercapto-undecanoic acid (MUA) on a typical SEIRA active gold surface allowed to immobilize cytochrome *c* through electrostatic interaction between the negatively charged MUA (at pH 7) and the positively charged protein surface.[14] This allowed us to obtain both a CV showing the reversible redox reaction of the heme and a differential SEIRAS spectrum revealing the changes in the vibrational modes of the protein backbone, certain amino acid side chains, and the heme. The electrode area was also increased by adding gold nanoparticles, so that the current measured in a CV experiment was increased.[15]

Different strategies have been employed to immobilize detergent solubilized membrane proteins on electrodes.[9] For example, a hydrophobic SAM of chemically modified alkanethiol can be used to adsorb the protein through its membrane domain.[16] Thiol-containing lipids were also used to create a lipid bilayer directly on the electrode, and the subsequent protein insertion into this bilayer is promoted by dialysis-based detergent removal. Other methods employed covalent attachment of the protein to SAM through chemical coupling between carboxylic acid and amine. Affinity-based immobilization of tagged proteins was also used, e.g., by using the streptavidin−biotin couple.

Concerning the respiratory chain enzyme complexes, mainly the adsorption of the cytochrome *c* oxidase on a gold electrode was studied.[17−19] One method was based on the affinity of a genetically introduced histidine-tag on the enzyme toward a nickel nitrilotriacetic acid (Ni-NTA) containing SAM. Once the protein was adsorbed, preformed liposomes were added and the detergent was removed through biobeads, reconstituting the native lipid bilayer. This approach is also possible for complex I, since the His-Tag labeled enzyme is available.[20] However, in this approach the NADH binding site of complex I (and the primary electron acceptor, FMN) may be too far away from the electrode surface to allow rapid electron transfer between the two (see Figure 1). In addition, owing to the size of complex I and since the SEIRA effect is limited to the first ∼10 nm from the gold surface,[21] it is possible that the IR absorption of some parts of the protein is not enhanced. As an alternative the immobilization of the natural substrate, reduced nicotinamide adenine dinucleotide, NADH, was thus probed. Currently, about 200 different enzymes have been reported which are known to catalyze reactions with these molecules as redox cofactors, and the generation of such an immobilization procedure would be useful for several proteins.[22]

Here we compare the two immobilization approaches for respiratory complex I and catalytically active fragments of the complex and probe them by SEIRAS and electrochemistry.

MATERIALS AND METHODS

Complex I and Fragments−Purification. Complex I was prepared from the overproducing *E. coli* strain BW25113/pBAD*nuo*/NuoF$_{His}$ as previously described.[20] The NADH dehydrogenase fragment was prepared from *E. coli* strain BL21(DE3)/pET11a/*nuoB-G*/*NuoF*$_C$.[23] and the subcomplex NuoEF from strain BL21(DE3)/pLacI/pETBlueI-NuoEF$_{His}$.[24] All preparation steps were carried out at 4 °C. A buffer of 20 mM MES/NaOH, 50 mM NaCl, pH 6.0 was used. For the preparation of complex I 0.01% of DDM was added.

ATR Cell. A configuration allowing the simultaneous acquisition of FTIR spectra in the attenuated total reflection (ATR) mode and the application of an electrochemical potential was built in analogy to ref 25. The ATR electro-

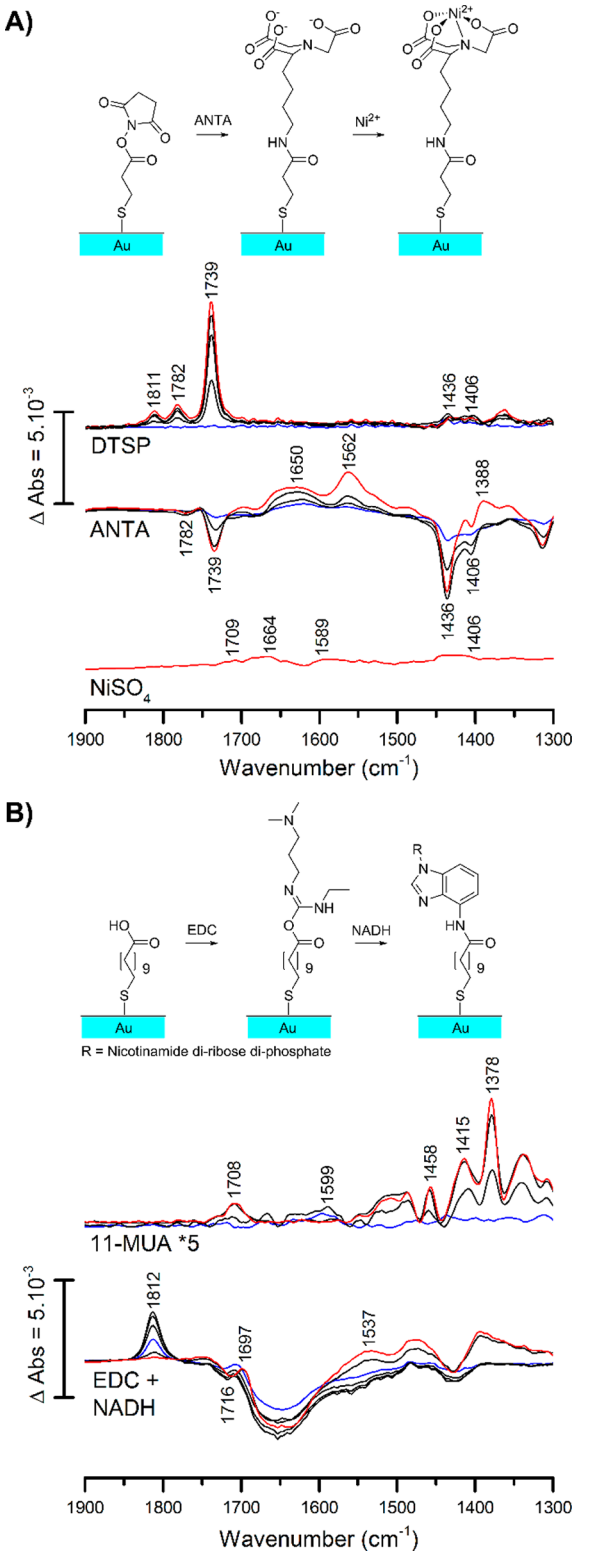

Figure 1. Presentation of the generation of the (A) Ni-NTA SAM and (B) NADH SAM on a gold layer as followed by SEIRAS. The spectra are presented as difference spectra, where the first reaction step was taken as a reference. The first spectra are shown by blue traces, the final spectra by red traces and the intermediate spectra by black traces. The spectra were recorded after 1, 5, 20, and 120 min for DTSP; 1, 6, 18, and 41 min for ANTA; 30 min for Ni^{2+}; 20 s and 1, 3, and 5 min for 11-MUA/mercaptohexanol; 2 and 10 min, 1, 5, and 10 h for EDC + NADH.

dx.doi.org/10.1021/bi500955a | *Biochemistry* 2014, 53, 6340−6347

chemical cell was made of a hemicylindrical "float zone" graded silicon prism (r = 1 cm, h = 2.5 cm, Korth) on which a glass cell was mounted. The glass cell (courtesy of Pr. Masatoshi Osawa, Hokkaido University) had 4 inlets, from which 2 were used to fit a Pt counter electrode and an Ag/AgCl reference electrode. A gold film deposited on the ATR crystal was used as working electrode. Upon assembly, the ATR crystal was coupled into the IR beam at an incident angle of 60° through a set of two gold-coated mirrors (Thorlabs) and a laboratory glass slide that was manually coated with gold. The optical path was fine-tuned through micrometric adjustments of the mirrors and the crystal positions to maximize the signal amplitude. All experiments were made within a Bruker Vertex 70 FTIR spectrometer (Globar source, KBr Beamsplitter, LN-MCT detector) at 6 mm aperture and 20 kHz scanner velocity.

Electroless Deposition of the Gold Film on the ATR Prism. For all experiments combining ATR-SEIRAS and electrochemistry, a hemicylindrical "float zone" graded silicon prism (r = 1 cm, h = 2.5 cm) was used (adapted from ref 26). Prior to the deposition of the gold film, the prism was polished with 0.3 μm alumina, rinsed with copious amounts of Millipore water, and then sonicated in water, acetone, and water. The prism was dried under an argon stream and immersed in 40% w/v NH_4F, rinsed, and dried again. It was heated up to 65 °C for 10 min, together with the plating solution. This solution was constituted of a 1:1:1 v/v/v mix of (A) 15 mM $NaAuCl_4$, (B) 150 mM Na_2SO_3, 50 mM $Na_2S_2O_3$, and 50 mM NH_4Cl, and (C) HF 2% w/v (total mix volume: 1 mL). Once the plating temperature reached, the prism was covered with the solution for 40 s and the reaction was stopped by washing the plating solution off with water, followed by Ar-stream drying. The resulting gold film was then tested for its electric conductance with a multimeter, the typical electric resistance of the layer as measured from one corner to another of the crystal should be around 15 Ω for a thickness of 50 nm.

Surface Modifications. *NADH-Mercapto-Undecanoic acid SAM.* For the NADH-SAM, the prism was first mounted in the electrochemical cell, and then covered with 500 μL ethanol. Then, a 1:10 mixture of 11-mercapto-undecanoic acid and 6-mercaptohexanol was added to a final concentration of 0.1 and 1 mM, respectively. The monolayer was allowed to self-assemble within 1 h. The prism was then rinsed with ethanol, dried with an argon stream, and covered with 1 mL Millipore water and *N*-(3-(dimethylamino)propyl)-*N*′-ethylcarbodiimide hydrochloride, that was added to a final concentration of 0.2 mM. After 5 min, 0.2 mM of NADH were added. The mixture was then allowed to stand overnight at room temperature. After completion, the prism was then rinsed with 5× Millipore water.

Ni-NTA SAM. The experimental procedure for the Ni-NTA SAM was adapted from ref 17. Prior to mounting in the electrochemical cell, the prism was covered with 1 $mg.mL^{-1}$ 3,3′-dithiodipropionic acid di(*N*-hydroxysuccinimide ester) (DTSP) in dry dimethyl sulfoxide and the monolayer was allowed to self-assemble for 1 h. The excess DTSP was then washed away with dry DMSO and the prism was dried under an argon stream. Once mounted in the measurement cell, it was then covered with 100 mM $N_{\alpha'},N_{\alpha''}$-bis(carboxymethyl)-L-lysine in 0.5 M K_2CO_3 at pH 9.8 for 3 h and then rinsed with water. Finally, the surface was incubated in 50 mM $NiSO_4$ for 1 h before being washed one last time with water.

Immobilization of Complex I and Reconstitution into a Lipid Bilayer. The modified gold layer was covered with 245 μL of MES buffer (50 mM 2-(*N*-morpholino)ethanesulfonic acid, 50 mM NaCl, pH 6.3) and 5 μL of 50 $mg.mL^{-1}$ purified *E. coli* complex I were added (final concentration: 1.9 μM). After 2 h, 70:25:5 phosphatidyl-ethanolamine (PE):phosphatidyl-glycerol (PG):cardiolipin (CL) liposomes were added to the mixture, and previously activated SM-2 Biobeads (BioRad) stored in MES buffer were deposited on the prism. The lipid bilayer was then allowed to form overnight and the biobeads and excess lipids were carefully washed off with MES buffer. The electrochemical cell was then filled with 20 mL MES buffer.

IR Spectroscopy. *Potential Induced Difference Spectroscopy of the Immobilized Enzymes.* With the proteins adsorbed on the gold surface, the ATR electrochemical cell was connected to a homemade potentiostat and the potential was cycled a few times between −700 mV and +200 mV vs Ag/AgCl 3 M KCl to ensure the correct functioning of the setup. Equilibration times for the oxidized and reduced states were set to 6 and 5 min, respectively. Twenty to thirty redox cycles were typically averaged to obtain the final spectrum.

Cyclic Voltammetry. In parallel to the IR spectroscopic experiments on the immobilized enzymes cyclic voltammetry experiments were conducted. The ATR electrochemical cell was connected to a Princeton applied research VersaSTAT4 potentiostat, and the potential was linearly swept from +300 mV to −650 mV and back at a scan rate of 0.02 $V.s^{-1}$.

RESULTS AND DISCUSSION

Validation of the Experimental Setup. To validate our experimental setup (i.e., correct mirror alignment, Au layer thickness, and electric connection) a small soluble protein from the respiratory chain, cytochrome *c*, was probed by electrochemically induced IR difference spectroscopy and cyclic voltammetry. The experiments were reported by Jiang et al.[14] and provided a good point of comparison. A SAM of 11-mercapto-undecanoic acid (MUA) was generated in ethanol for 90 min on the gold coated ATR crystal, and then the surface was dried under an N_2 stream, immersed in phosphate buffer, and cytochrome *c* was added to a final concentration of 2 μM. The resulting IR difference spectrum and the cyclovoltammogram are shown in the Supporting Information (Figure S1). The fully oxidized *minus* fully reduced spectrum and the cyclovoltammogram of adsorbed Cyt_c were virtually identical to those from Jian et al.,[14] confirming that the gold layer had an appropriate thickness, that the IR beam incidence angle on the prism was correct, and that the current was effectively transferred from the electrodes through the gold to the protein. The setup was thus ready for exploration of immobilization methods for complex I.

Generation of the Different SAM and Immobilization of Complex I. *Ni-NTA SAM.* The first method to immobilize complex I is based on the same strategy as previously reported for cytochrome *c* oxidase, i.e., the affinity-based adsorption of a His-tagged protein on a Ni-NTA SAM.[17,27] The His-tag was attached to the N-terminus of subunit NuoF, so that the enzyme would be immobilized through the tip of the peripheral arm. The Ni-NTA SAM was prepared through the generation of a SAM containing an O-succinimide ester, which was coupled to nitrilotriacetic acid and chelated with Ni^{2+}.

In order to monitor the formation of the Ni-NTA SAM, an IR analysis shown in Figure 1A was made. The data are shown as difference spectra, with the respective background spectra being taken in the presence of the respective solvents. For the adsorption and subsequent chemical modification of the DTSP

dx.doi.org/10.1021/bi500955a | *Biochemistry* 2014, 53, 6340−6347

SAM, the signals from the DMSO solvent at 1436 and 1406 cm^{-1} overlap signals from DTSP and ANTA around these positions, but the marker bands of DTSP ($\nu(C{=}O)_{succinimide}$ and $\nu(C{=}O)_{ester}$ at 1811/1782 and 1739 cm^{-1}, respectively) and ANTA ($\nu_s(COO^-)$ at 1388 cm^{-1}) are also evident. The amide bond formation is seen from the arising peptide's amide I and II modes at ~1650 (broad) and 1562 cm^{-1}. The Ni^{2+} chelation changed not only the $\nu_{as}(COO^-)$ and $\nu_s(COO^-)$ modes of ANTA (1589 and 1436 cm^{-1}, respectively), but also two bands at 1709 and 1664 cm^{-1} which could represent parasite Ni^{2+} chelation by the amide. However, this effect was not removed even after extensive rinsing, so this alternative is less likely. A signal at 1284 cm^{-1} (not shown here) may represent the $\nu(C{-}N)$ mode of the tertiary amine, which is also involved in the chelation. The formation of the Ni-NTA SAM took place within 2 h and was highly reproducible. The immobilization strategy is summarized in the scheme in Figure 2.

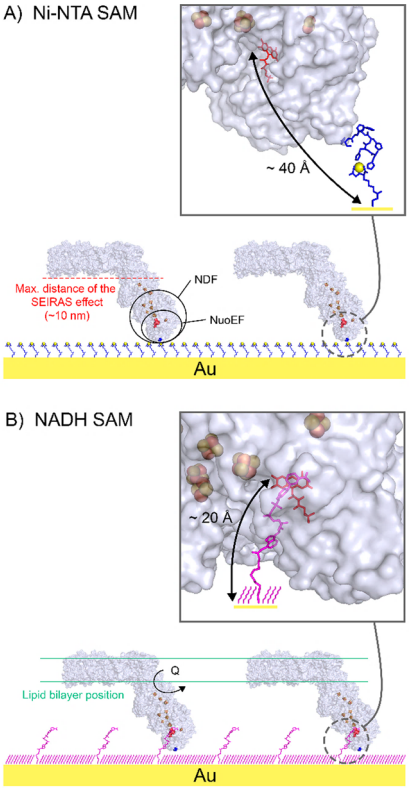

Figure 2. Strategies for the oriented immobilization of complex I. The components of the SAMs are represented as follows: Complex I as a light blue surface, FMN as red sticks, FeS clusters as brown spheres, Ni-NTA and His-tag as blue sticks with Ni atom in yellow, and 6-mercaptohexanol and 11-mercapto-undecanoic acid coupled to NADH as magenta sticks. The putative position of the lipid bilayer after reconstitution is indicated by the green lines. PDB ID used for representation: 4HEA, except for inset in (B) where 3IAM was used.

NADH-SAM. In the second approach the NADH substrate was attached to a preformed SAM, in order to reduce the distance between the gold surface and the FMN, and to allow a direct and rapid electron input to the FMN cofactor, which is the first electron acceptor. The covalent immobilization of NADH was obtained through a rather simple process. The alkanethiols used to create the SAM contain a carboxylic acid which forms a peptide bond with the NADH adenine-amine when a cross-linking agent is added. To avoid steric hindrance for the correct insertion of NADH into the binding pocket, a mixed SAM composed of a longer-chain acid and short-chain alcohols have been used.

In Figure 1B, the steps for the assembly of the NADH-SAM are shown together with the reactions as followed by IR difference spectroscopy. The first step, i.e., the self-assembly of a MUA:6-mercaptohexanol 1:10 monolayer, is rapid (5 min), and the signals at 1708 cm^{-1} ($\nu(C{=}O)COOH$), 1599 and 1415/1378 cm^{-1} ($\nu_s(COO^-)$ and $\nu_{as}(COO^-)$) indicate that the acid is present in a mixture of protonated and deprotonated forms. The adsorption of the 6-mercaptohexanol is not specifically seen here since the reference spectrum was taken in ethanol, which overlaps the alcohol group vibrations. The increase of the number of alkyl groups near the surface is shown by the band at1458 cm^{-1}.

The coupling of NADH with MUA produced complex spectra due to the number of reactants, intermediates, and products involved here. For example, water (buffer), NADH, urea, and the NADH-MUA amide all show broad IR absorption around 1650 ± 30 cm^{-1} and overlap, so that no direct conclusion can be drawn for the formation of the amide. By recording a reference spectrum in the presence of EDC and immediately after addition of NADH, the evolution of the reaction could nevertheless be followed. A signal at 1812 cm^{-1} was tentatively attributed to the reaction intermediate shown in Figure 2B. This signal might also represent an anhydride, which is from an alternative reaction path, but this is less likely since anhydrides are unstable in water. The band rises quickly (10 min) and then diminishes slowly before disappearing after 10 h. Concomitantly, two peaks appear at 1697 and 1537 cm^{-1}, which could represent the amide I and II modes of the MUA-NADH peptide. Thus, we suggest that the coupling was complete after 10 h. The slow reaction kinetics are consistent with the low reactivity of the amine from the NADH's adenine moiety due to the delocalization of its lone pair over the aromatic ring. Side reactions might also happen during the peptide coupling, as suggested by a negative peak below 1250 cm^{-1}. This signal could represent reaction of the phosphate from NADH (or simply, its protonation), but could also be due to baseline instabilities that were sometimes observed in this spectral region. The sample was then extensively rinsed to probe the stability of the SAM.

After generation of the SAMs, complex I was adsorbed at their surface. The process was followed by IR spectroscopy as shown in Figure 3. On both SAMs, the amide I and II modes of complex I were clearly visible, but their shape, position, and intensity ratio varied. Slight differences in thickness and nanostructure of the gold layer may partially explain these variations.[28] However, the most straightforward explanation of these differences is a different orientation of the protein with respect to the surface, since amide modes are highly orientation dependent.[29] The insets in Figure 3 showing the deconvolution of the amide I band further points toward a change of protein orientation between the two SAMs. Due to the size of the adsorbed complex, it was not possible to determine the exact orientation of the protein as can be done for smaller molecules. The intensity of the amide bands progressively increased before stabilizing after approximately 2 h, indicating that during this period a certain organization of the protein layer occurs. For both SAMs, complex I is tightly adsorbed on the surface, as the amide signals persisted after rinsing of the crystal with buffer to remove excess protein.

dx.doi.org/10.1021/bi500955a | *Biochemistry* 2014, 53, 6340−6347

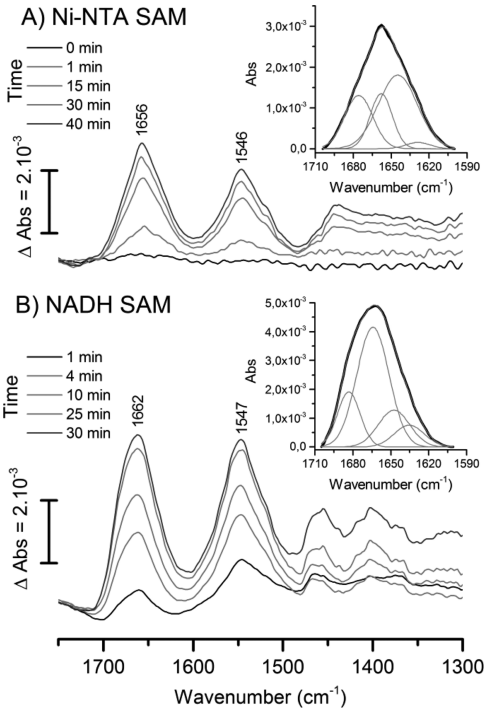

Figure 3. Evolution of the adsorption of complex I on the modified surface followed by SEIRAS for the (A) Ni-NTA SAM and (B) NADH SAM. The insets show the deconvoluted amide I band.

Probing the Electrochemically Induced Reaction of the Immobilized Complex I through SEIRAS and CV. The electrochemically induced FTIR difference spectra were all fully reversible, be it for the SAM alone or in the presence of complex I. First, the oxidized minus reduced IR difference spectra of the NADH-SAM and the Ni-NTA-SAM before adsorption of Complex I were obtained (see Figure S2, Supporting Information). A large negative peak at 1650/1642 cm^{-1} was attributed to interfacial water molecule reorganization upon redox reaction. The reorganization of interfacial water[30−32] upon the applied potential was observed in all electrochemically induced IR difference spectra. This was reported in studies on the reorganization of lipid layers on gold surfaces by means of SEIRAS upon an applied potential.[33] The oxidized minus reduced spectra of both SAMs with adsorbed Complex I were then recorded. They boasted a similar, almost featureless (except for the water band around 1650 cm^{-1}) differential IR spectrum. In the spectrum of the Ni-NTA-SAM, a shoulder probably representing a carbonyl mode was seen at 1677 cm^{-1}. For the following data the contribution of the water was thus subtracted in order to highlight the redox induced reorganization of the protein.

The CV of the two SAMs looked identical at the first glimpse (see Supporting Information Figure S3); however, it is noted that the CV evolved after several redox-cycles. For the NADH-SAM, it reverted almost to that of bare gold, where oxygen reacts at the surface, with a signal at about −350 mV. For the Ni-NTA-SAM, in addition to the signal at −350 mV a second reductive peak was seen at −545 mV. This probably represents partial desorption of the SAM when exposed to reducing potentials and reduction of Ni^{2+} to Ni^0 (E^0 = −250 mV vs SHE). This reactivity might complicate analysis of the CV from further experiments. On the other hand, the redox-induced difference spectra did not show any evidence of SAM and protein desorption during the course of the experiments. This was carefully taken into account when analyzing the complex I data shown below.

The oxidized minus reduced IR spectrum of complex I immobilized on the NADH-SAM where water contribution was subtracted is shown in Figure 4A. The peak at 1538 cm^{-1} is

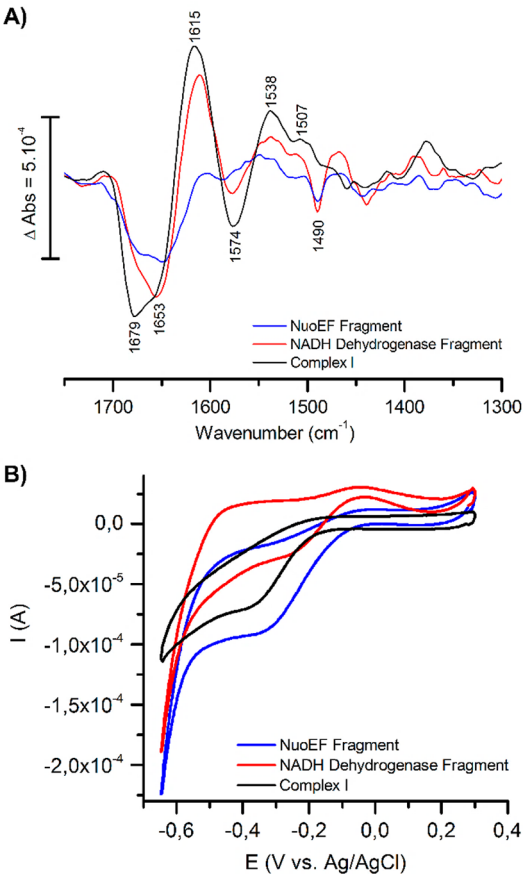

Figure 4. (A) IR double difference spectra obtained by subtracting the IR difference spectra for the SAM alone from the IR difference of the NuoEF complex (blue line), the NADH dehydrogenase fragment (red line), and complex I from *E. coli* (black line), and (B) CV of the NuoEF complex (blue line), the NADH dehydrogenase fragment (red line), and complex I from *E. coli* (black line) adsorbed on the NADH-SAM.

partially attributed to ν(C═C) mode of the FMN cofactor together with the contribution from the amide II vibration of the backbone. The intense bands at 1679 and 1615 cm^{-1} include contributions from β-sheets/turns and the signal at 1653 cm^{-1} most likely represents those of α-helices or randomly structured amide backbones.

Owing to the considerable size of complex I (ca. 180 × 170 × 60 $Å^3$) and the decay of the SEIRA effect with increasing distance from the surface,[12,21,34] it was not clear whether the membrane arm of the complex located at some distance from the surface (Figure 2) contributed to the spectrum (Figure 4A). To probe this, fragments of the complex lacking the membrane arm were adsorbed through the same method on the NADH-SAM and their ox-red spectra were compared to those of the entire enzyme (Figure 4A, red and blue line). The NADH dehydrogenase fragment comprises subunits NuoE, F, and G and contains the FMN and all but three Fe−S clusters. Subcomplex NuoEF from *Aquifex aeolicus* is made up of

dx.doi.org/10.1021/bi500955a | *Biochemistry* 2014, 53, 6340−6347

subunits NuoE and F harboring the FMN and two Fe−S clusters.

The oxidized-minus-reduced IR difference spectra of the fragments show signals at similar positions as for the entire complex; however, their intensities vary. The major part of the complex I spectrum seems to arise from the dehydrogenase fragment (as seen for complex I in solution in the thin-layer electrochemical cell,[35] with additional absorptions at 1679 and 1615 cm^{-1}, and a more intense amide I mode, that can tentatively be attributed to the conformational movements in the membrane domain, discussed before[35−37]). However, the variations of the Au layer properties or a different orientation of the entire complex compared to that of the fragments might also be at the origin of these differences. The signals at 1733, 1574, and 1407 cm^{-1} are attributed to protonation reactions of carboxylic acids from complex upon reduction in direct comparison to the signals expected for the isolated amino acids.[38,39]

Figure 4B shows the CVs of the entire complex I (black line), the NuoEF (blue line), and the dehydrogenase fragment, respectively (red line). A similar shape as for the NADH-SAM alone is found describing a kinetically slow reaction at the electrode, as can be deduced from the shape of the CV that included the negative reduction peak, but no positive oxidation peak. It is noted that, because the cofactors are buried within the protein, it is difficult to immobilize these proteins in such a way that they can perform direct electron transfer with satisfactory electron transfer rates.

The different fragments show different reduction potentials; this may be attributed not only to the different content of cofactors present, but also to the eventually different orientation of each of the three samples. The intrinsic redox potentials of the complex I cofactors range from ca. −150 to −400 mV vs SHE; the observed potential is found within this range.[24,40] The signal seen is most likely a mixture of the protein and the NADH-SAM. Even if a densely packed protein monolayer was formed, the surface coverage of complex I would be quite low due to its size (1.6×10^{-12} mol/cm^2 in the best case scenario).

Similarly, complex I on the Ni-NTA-SAM was also probed and compared to the NADH-SAM. Above 1500 cm^{-1}, the signals observed were similar, although less intense for the Ni-NTA-SAM. The corresponding CV were also similar to those obtained with the NADH-SAM. No influence from the distance is thus observed.

Lipid Reconstitution. The adsorbed complex I was reconstituted in lipids by addition of preformed PE:PG:CL liposomes and subsequent detergent removal with Biobeads. The process was monitored by IR difference spectroscopy (Supporting Information Figure S4). The presence of lipids is seen by the increase of the signals at 1729 (NADH-SAM) and 1725 (Ni-NTA-SAM) cm^{-1}. For both SAMs, the insertion of complex I into a lipid bilayer also caused variations within the amide I region (+1671 cm^{-1} in the NADH-SAM, −1655 cm^{-1} in the Ni-NTA-SAM) reflecting structural (re)organization of the protein layer in relation to the surface.

Figure 5A shows the oxidized minus reduced IR difference spectra in the presence and absence of the lipids. Interestingly an overall diminution of the signals of complex I was observed when the enzyme was reconstituted with lipids on a NADH-SAM, whereas the contrary occurred on a Ni-NTA-SAM. This may indicate that the Ni-NTA is more favorably oriented for the complex reconstituted in lipids.

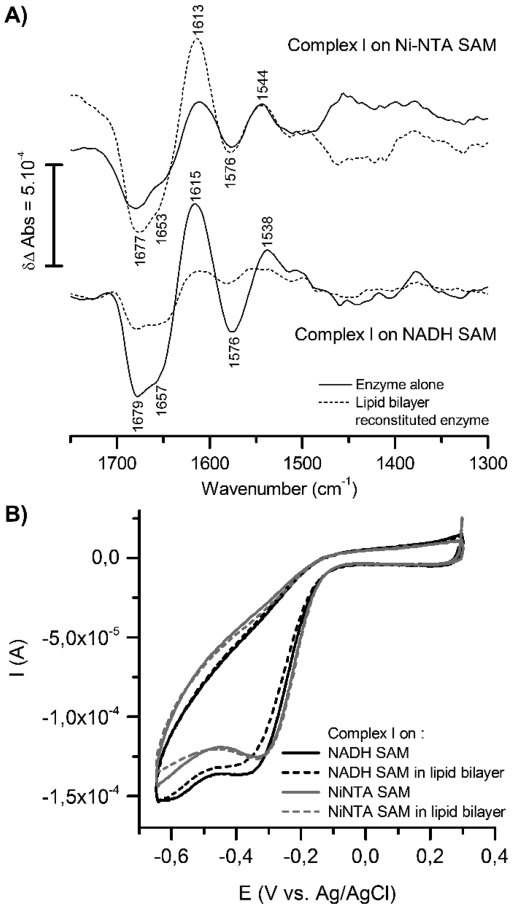

Figure 5. (A) IR double difference spectra obtained by subtracting the IR difference spectra for the SAM alone from the IR difference of complex I and (B) CV of the adsorbed complex I in detergent (full line) and reconstituted into a lipid bilayer (dotted line) for each SAM.

The CVs after and before lipid addition (Figure 5B) are very similar. A very small diminution of the reductive peak in the NADH-SAM is noted, which was less pronounced in the Ni-NTA-SAM. The effect was significantly smaller than expected, since the presence of lipids is known to influence the electrochemically induced catalytic properties of the enzyme.[41,42] However, lipids will not influence the electron transfer process; only the conformational changes in the protein that are highly discussed are a crucial part of the catalytic proton pumping activity.

■ CONCLUSIONS

An experimental approach allowing combined SEIRAS and CV experiments on protein films was successfully set up. A stable (against mechanical forces such as rinsing) layer of the adsorbed enzyme was formed, but on the other hand its functional probing through SEIRAS and CV was complicated by various factors. However, the long-term stability of the thiol SAM when exposed to reducing potentials below −500 mV (about −700 mV vs SHE) was observed to be low. Interestingly, both immobilization procedures, via the His-tag and the NADH-SAM, worked, indicating that the distance from the surface was still satisfactory for electron transfer. While the exact orientation of complex I with respect to the surface is unknown, the experiments with the dehydrogenase fragment and subcomplex NuoEF indicated that the major part of the IR

dx.doi.org/10.1021/bi500955a | Biochemistry 2014, 53, 6340−6347

signals seen for the entire complex arise from the dehydrogenase fragment. Additional signals are seen when the entire complex I is studied, indicating that the size of complex I is not a barrier to its study by SEIRAS.

■ ASSOCIATED CONTENT

Supporting Information

Control SEIRAS experiments on cytochrome *c*, adsorbed on a 11-mercaptoundecanoic acid SAM. Control experiments on SAM alone, and infrared data on complex I in lipids. This material is available free of charge via the Internet at http://pubs.acs.org.

■ AUTHOR INFORMATION

Corresponding Author

*E-mail: hellwig@unistra.fr.

Present Address

Sébastien Kriegel, Laboratoire d'Electrochimie Moléculaire, Université Paris Diderot, UMR CNRS 7591, 15, rue Jean-Antoine de Baïf, 75205 Paris Cedex 13, France.

Author Contributions

The manuscript was written through contributions of all authors. All authors have given approval to the final version of the manuscript.

Notes

The authors declare no competing financial interest.

■ ACKNOWLEDGMENTS

P.H. and S.K. are grateful to the Région Alsace, the Centre International de Recherche aux Frontières de la Chimie (FRC), CNRS, the Japanese Society for the Promotion of Science (JSPS). T.F. acknowledges financial support from the DFG. M.O. acknowledges financial support from JSPS (KAKENHI Grant Number 24550143).

■ ABBREVIATIONS

SEIRAS, surface-enhanced IR absorption spectroscopy; SAM, self-assembled monolayer; ANTA, amino-nitrilotriacetic acid ($N\alpha'$,$N\alpha''$-bis(carboxymethyl)-L-lysine); DTSP, dithiobis-(succinimidylpropionate); Histag, hexahistidine tag; MUA, 11-mercaptoundecanoic acid; NADH, nicotinamide adenine dinucleotide (H)

■ REFERENCES

(1) Brandt, U. (2013) Inside view of a giant proton pump. *Angew. Chem., Int. Ed. 52*, 7358−7360.

(2) Leif, H., Weidner, U., Berger, A., Spehr, V., Braun, M., van Heek, P., Friedrich, T., Ohnishi, T., and Weiss, H. (1993) Escherichia coli NADH dehydrogenase I, a minimal form of the mitochondrial complex I. *Biochem. Soc. Trans. 21*, 998−1001.

(3) Carroll, J., Fearnley, I. M., Shannon, R. J., Hirst, J., and Walker, J. E. (2003) Analysis of the subunit composition of complex I from bovine heart mitochondria. *Mol. Cell. Proteomics 2*, 117−126.

(4) Baradaran, R., Berrisford, J. M., Minhas, G. S., and Sazanov, L. A. (2013) Crystal structure of the entire respiratory complex I. *Nature 494*, 443−448.

(5) Zickermann, V., Kerscher, S., Zwicker, K., Tocilescu, M. A., Radermacher, M., and Brandt, U. (2009) Architecture of complex I and its implications for electron transfer and proton pumping. *Biochim. Biophys. Acta 1787*, 574−583.

(6) Ataka, K., and Heberle, J. (2006) Use of surface enhanced infrared absorption spectroscopy (SEIRA) to probe the functionality of a protein monolayer. *Biopolymers 82*, 415−419.

(7) Ataka, K., Stripp, S. T., and Heberle, J. (2013) Surface-enhanced infrared absorption spectroscopy (SEIRAS) to probe monolayers of membrane proteins. *Biochim. Biophys. Acta - Biomembranes 1828*, 2283−2293.

(8) Melin, F., and Hellwig, P. (2013) Recent advances in the electrochemistry and spectroelectrochemistry of membrane proteins. *Biol. Chem. 394*, 593−609.

(9) Murgida, D. H., Hildebrandt, P., Todorovic, S. (2010) Immobilized redox proteins: mimicking basic features of physiological membranes and interfaces, In *Biomimetics, Learning from Nature* (Mukherjee, A., Ed.) pp 21−48, InTech.

(10) Naumann, R. L. C., Nowak, C., and Knoll, W. (2011) Proteins in biomimetic membranes: promises and facts. *Soft Matter 7*, 9535−9548.

(11) Butt, J., and Armstrong, F. (2008) Voltammetry of Adsorbed Redox Enzymes: Mechanisms in The Potential Dimension, In *Bioinorganic Electrochemistry* (Hammerich, O., and Ulstrup, J., Eds.), pp 91−128, Springer, Netherlands.

(12) Osawa, M. (1997) Dynamic processes in electrochemical reactions studied by surface-enhanced infrared absorption spectroscopy (SEIRAS). *Bull. Chem. Soc. Jpn. 70*, 2861−2880.

(13) Ly, H. K., Sezer, M., Wisitruangsakul, N., Feng, J.-J., Kranich, A., Millo, D., Weidinger, I. M., Zebger, I., Murgida, D. H., and Hildebrandt, P. (2011) Surface-enhanced vibrational spectroscopy for probing transient interactions of proteins with biomimetic interfaces: electric field effects on structure, dynamics and function of cytochrome c. *FEBS J. 278*, 1382−1390.

(14) Jiang, X. U., Ataka, K., and Heberle, J. (2008) Influence of the molecular structure of carboxyl-terminated self-assembled monolayer on the electron transfer of cytochrome c adsorbed on an an electrode: In situ observation by surface-enhanced infrared absorption spectroscopy. *J. Phys. Chem. C 112*, 813−819.

(15) Murata, K., Kajiya, K., Nukaga, M., Suga, Y., Watanabe, T., Nakamura, N., and Ohno, H. (2010) A simple fabrication method for three-dimensional gold nanoparticle electrodes and their application to the study of the direct electrochemistry of cytochrome c. *Electroanalysis 22*, 185−190.

(16) Kozuch, J., Steinem, C., Hildebrandt, P., and Millo, D. (2012) Combined electrochemistry and surface-enhanced infrared absorption spectroscopy of gramicidin A incorporated into tethered bilayer lipid membranes. *Angew. Chem., Int. Ed. 51*, 8114−8117.

(17) Ataka, K., Giess, F., Knoll, W., Naumann, R., Haber-Pohlmeier, S., Richter, B., and Heberle, J. (2004) Oriented attachment and membrane reconstitution of His-tagged cytochrome c oxidase to a gold electrode: in situ monitoring by surface-enhanced infrared absorption spectroscopy. *J. Am. Chem. Soc. 126*, 16199−16206.

(18) Nowak, C., Schach, D., Gebert, J., Grosserueschkamp, M., Gennis, R. B., Ferguson-Miller, S., Knoll, W., Walz, D., and Naumann, R. L. C. (2010) Oriented immobilization and electron transfer to the cytochrome c oxidase. *J. Solid State Electrochem. 15*, 105−114.

(19) Todorovic, S., Verissimo, A., Wisitruangsakul, N., Zebger, I., Hildebrandt, P., Pereira, M. M., Teixeira, M., and Murgida, D. H. (2008) SERR-spectroelectrochemical study of a cbb3 oxygen reductase in a biomimetic construct. *J. Phys. Chem. B 112*, 16952−16959.

(20) Pohl, T., Uhlmann, M., Kaufenstein, M., and Friedrich, T. (2007) Lambda red-mediated mutagenesis and efficient large scale affinity purification of the Escherichia coli NADH:ubiquinone oxidoreductase (complex I). *Biochemistry 46*, 10694−10702.

(21) Osawa, M., and Ikeda, M. (1991) Surface-enhanced infrared absorption of p-nitrobenzoic acid deposited on silver island films: Contributions of electromagnetic and chemical mechanisms. *J. Phys. Chem. 95*, 9914−9919.

(22) Kerscher, S., Dröse, S., Zickermann, V., and Brandt, U. (2008) The Three Families of Respiratory NADH Dehydrogenases, In *Bioenergetics* (Schäfer, G., and Penefsky, H., Eds.) pp 185−222, Springer, Berlin.

(23) Bungert, S., Krafft, B., Schlesinger, R., and Friedrich, T. (1999) One-step purification of the NADH dehydrogenase fragment of the

Escherichia coli complex I by means of Strep-tag affinity chromatography. *FEBS Lett. 460*, 207−211.
(24) Kohlstadt, M., Dorner, K., Labatzke, R., Koc, C., Hielscher, R., Schiltz, E., Einsle, O., Hellwig, P., and Friedrich, T. (2008) Heterologous production, isolation, characterization and crystallization of a soluble fragment of the NADH:ubiquinone oxidoreductase (complex I) from Aquifex aeolicus. *Biochemistry 47*, 13036−13045.
(25) Ataka, K., and Heberle, J. (2004) Functional vibrational spectroscopy of a cytochrome c monolayer: SEIDAS probes the interaction with different surface-modified electrodes. *J. Am. Chem. Soc. 126*, 9445−9457.
(26) Miyake, H., Ye, S., and Osawa, M. (2002) Electroless deposition of gold thin films on silicon for surface-enhanced infrared spectroelectrochemistry. *Electrochem. Commun. 4*, 973−977.
(27) Schartner, J., Güldenhaupt, J., Mei, B., Rögner, M., Muhler, M., Gerwert, K., and Kötting, C. (2013) Universal method for protein immobilization on chemically functionalized germanium investigated by ATR-FTIR difference spectroscopy. *J. Am. Chem. Soc. 135*, 4079−4087.
(28) Guo, H., Kimura, T., and Furutani, Y. (2013) Distortion of the amide-I and -II bands of an α-helical membrane protein, pharaonis halorhodopsin, depends on thickness of gold films utilized for surface-enhanced infrared absorption spectroscopy. *Chem. Phys. 419*, 8−16.
(29) Vigano, C., Manciu, L., Buyse, F., Goormaghtigh, E., and Ruysschaert, J. M. (2000) Attenuated total reflection IR spectroscopy as a tool to investigate the structure, orientation and tertiary structure changes in peptides and membrane proteins. *Biopolymers 55*, 373−380.
(30) Herrwerth, S., Eck, W., Reinhardt, S., and Grunze, M. (2003) Factors that determine the protein resistance of oligoether self-assembled monolayers - Internal hydrophilicity, terminal hydrophilicity, and lateral packing density. *J. Am. Chem. Soc. 125*, 9359−9366.
(31) Hower, J. C., He, Y., and Jiang, S. Y. (2008) A molecular simulation study of methylated and hydroxyl sugar-based self-assembled monolayers: Surface hydration and resistance to protein adsorption. *J. Chem. Phys. 129*, 215101.
(32) Osawa, M., Tsushima, M., Mogami, H., Samjeské, G., and Yamakata, A. (2008) Structure of water at the electrified platinum−water interface: a study by surface-enhanced infrared absorption spectroscopy. *J. Phys. Chem. C 112*, 4248−4256.
(33) Uchida, T., Osawa, M., and Lipkowski, J. (2014) SEIRAS studies of water structure at the gold electrode surface in the presence of supported lipid bilayer. *J. Electroanal. Chem. 716*, 112−119.
(34) Osawa, M. (2001) Surface-Enhanced Infrared Absorption, In *Near-Field Optics and Surface Plasmon Polaritons* (Kawata, S., Ed.) pp 163−187, Springer, Berlin.
(35) Hellwig, P., Scheide, D., Bungert, S., Mantele, W., and Friedrich, T. (2000) FT-IR spectroscopic characterization of NADH:ubiquinone oxidoreductase (complex I) from Escherichia coli: oxidation of FeS cluster N2 is coupled with the protonation of an aspartate or glutamate side chain. *Biochemistry 39*, 10884−10891.
(36) Hellwig, P., Stolpe, S., and Friedrich, T. (2004) Fourier transform infrared spectroscopic study on the conformational reorganization inEscherichia coli complex I due to redox-driven proton translocation. *Biopolymers 74*, 69−72.
(37) Friedrich, T., and Hellwig, P. (2010) Redox-induced conformational changes within the Escherichia coli NADH ubiquinone oxidoreductase (complex I): An analysis by mutagenesis and FT-IR spectroscopy. *Biochim. Biophys. Acta - Bioenergetics 1797*, 659−663.
(38) Barth, A. (2007) Infrared spectroscopy of proteins. *Biochim. Biophys. Acta 1767*, 1073−1101.
(39) Wolpert, M., and Hellwig, P. (2006) Infrared spectra and molar absorption coefficients of the 20 alpha amino acids in aqueous solutions in the spectral range from 1800 to 500 cm^{-1}. *Spectrochim. Acta, Part A 64*, 987−1001.
(40) Euro, L., Bloch, D. a., Wikström, M., Verkhovsky, M. I., and Verkhovskaya, M. (2008) Electrostatic interactions between FeS clusters in NADH:ubiquinone oxidoreductase (Complex I) from Escherichia coli. *Biochemistry 47*, 3185−3193.
(41) Sharpley, M. S., Shannon, R. J., Draghi, F., and Hirst, J. (2006) Interactions between phospholipids and NADH:ubiquinone oxidoreductase (complex I) from bovine mitochondria. *Biochemistry 45*, 241−248.
(42) Drose, S., Zwicker, K., and Brandt, U. (2002) Full recovery of the NADH:ubiquinone activity of complex I (NADH:ubiquinone oxidoreductase) from Yarrowia lipolytica by the addition of phospholipids. *Biochim. Biophys. Acta 1556*, 65−72.